

STOCKHOLM UNIVERSITY

Doctoral Studies in Physics

Licensiate Thesis

Search for $\tilde{\chi}^0$ in Mono-jet Final States with the ATLAS Experiment



Advisor:

dott. Christophe CLEMENT

Co-Supervisor:

dott. David MILSTEAD

Candidate:

Gabriele BERTOLI

DECEMBER 12, 2015

Acknowledgments

Contents

Acknowledgments	IV
1 Theoretical overview	1
1.1 The Standard Model of particle physics	1
1.2 The Standard Model	1
1.2.1 Electro-Weak Symmetry Group	1
1.2.2 Electro-Weak Interactions	3
1.3 The Higgs mechanism	5
1.3.1 Non Abelian Spontaneously Broken Symmetry	5
1.3.2 The Higgs Mechanism	6
1.3.3 Masses for the W^\pm and Z^0 Gauge Bosons	8
1.4 The hierarchy problem and naturalness	8
2 Experimental apparatus	11
2.1 The large hadron collider	11
2.2 The ATLAS detector	11
2.2.1 The inner detector	11
2.2.2 The calorimeter	12
2.2.3 The muon spectrometer	13
2.2.4 The forward detectors	13
2.2.5 Track reconstruction	14
2.2.6 The trigger system	14
3 Physical objects reconstruction	15
3.1 Lepton reconstruction and identification	15
3.1.1 Primary Vertex	15
3.1.2 Overlap removal	15
3.1.3 Electrons	15
3.1.4 Jets	16
3.1.5 Missing transverse energy	16
3.1.6 Muons	16
4 The Monojet signature	17
4.1 Motivation	17
4.2 Event Selection	18
Appendix A Some title	19
Bibliography	19

List of Tables

1.1	Weak Isospin and Hypercharge Quantum Numbers of Leptons and Quarks	3
3.1	Monojet electron definition	16

List of Figures

2.1	Schematic view of a charged track of 10 GeV p_T that traverses the different ID sub-detectors. After traversing the beryllium pipe, the track passes through the three cylindrical silicon-pixel layers, the four layers of silicon-microstrip sensors (SCT) and the approximately 36 straws contained in the TRT within their support structure.	12
2.2	Cut-away view of the ATLAS calorimeter system.	13
2.3	Cut-away view of the ATLAS muon spectrometer.	14
4.1	17

*Si sta,
come d'autunno,
sugli alberi,
le foglie*

[G. UNGARETTI, Soldati]

Introduction

Chapter 1

Theoretical overview

1.1 The Standard Model of particle physics

1.2 The Standard Model

The *Standard Model* (SM) is a theoretical model which describes the elementary constituents of matter and their interactions. Up to now, we discovered four kind of different interactions, the *electromagnetic*, the *gravitational*, the *strong* and the *electro-weak interaction*; excluding gravity, all of them are described by means of a *quantum field gauge theory*.

The Standard Model is the collection of these gauge theories, it is based on the gauge symmetry group $SU(3)_C \times SU(2)_L \times U(1)_Y$ where $SU(3)_C$ is the symmetry group of the *Quantum Chromo-Dynamics* (QCD), the “C” subscript stand for *color charge* which is the conserved charge in the strong interaction. The $SU(2)_L$ is the weak isotopic spin group acting on *left-handed* doublet of fermions while the $U(1)_Y$ group is the *hypercharge* symmetry group of the *right-handed* fermion singlets. Together $SU(2)_L \times U(1)_Y$ form the electro-weak symmetry group.

The Standard Model also contains and (sometimes) predicts the existence of *elementary particles* that interacts between them via the forces mentioned above. The matter constituents are called *fermions*, the interaction are mediated by other particles called *gauge bosons*. Fermions are further categorized into *quark* and *leptons* and are the true fundamental constituents of matter; the gauge bosons arise by means of symmetry property of the Standard Model symmetry group.

The existence of all the leptons, quarks and gauge bosons is confirmed by experimental tests. Among the bosons, the Higgs boson is peculiar because, unlike the others, it is not associated with any interaction, instead is postulated as a consequence of the *spontaneously broken symmetry* of the electroweak sector which is the property, responsible of giving mass to all the elementary particles and the weak gauge bosons.

1.2.1 Electro-Weak Symmetry Group

We can now see how to find out the weak interaction symmetry group, to this end, let us start by writing out the *Hamiltonian*

$$H_{weak} = \frac{4G_F}{\sqrt{2}} J_\mu^\dagger J^\mu \quad (1.2.1)$$

where

$$\begin{aligned} J_\mu &\equiv J_\mu^{(+)} = \bar{\psi}_{\nu_e} \gamma_\mu \frac{1}{2} (1 - \gamma_5) \psi_e \equiv \bar{\nu}_{eL} \gamma_\mu e_L \\ J_\mu^\dagger &\equiv J_\mu^{(-)} = \bar{\psi}_e \gamma_\mu \frac{1}{2} (1 - \gamma_5) \psi_{\nu_e} \equiv \bar{e}_L \gamma_\mu \nu_{eL} \end{aligned} \quad (1.2.2)$$

to easy the notation, let us write

$$\chi_L = \begin{pmatrix} \nu_{eL} \\ e_L^- \end{pmatrix} \equiv \begin{pmatrix} \nu_e \\ e^- \end{pmatrix} \quad (1.2.3)$$

and using the Pauli matrices

$$\tau_\pm = \frac{1}{2}(\tau_1 \pm i\tau_2) \quad (1.2.4)$$

we have

$$\begin{aligned} J_\mu^{(+)} &= \bar{\chi}_L \gamma_\mu \tau_+ \chi_L \\ J_\mu^{(-)} &= \bar{\chi}_L \gamma_\mu \tau_- \chi_L \end{aligned} \quad (1.2.5)$$

by introducing a “neutral” current

$$J_\mu^{(3)} = \bar{\chi}_L \gamma_\mu \frac{\tau_3}{2} \chi_L = \frac{1}{2} \bar{\nu}_L \gamma_\mu \nu_L - \frac{1}{2} \bar{e}_L \gamma_\mu e_L \quad (1.2.6)$$

we have a “triplet” of currents

$$J_\mu^i = \bar{\chi}_L \gamma_\mu \frac{\tau_i}{2} \chi_L. \quad (1.2.7)$$

Now if we pick up an $SU(2)_L$ transformation

$$\chi_L(x) \rightarrow \chi'_L(x) = e^{i\vec{\varepsilon} \cdot \vec{T}} \chi_L(x) = e^{i\vec{\varepsilon} \cdot \frac{\vec{\tau}}{2}} \chi_L(x), \quad (1.2.8)$$

where $T_i = \tau_i/2$ are the $SU(2)_L$ generators, and think the χ_L as the *fundamental representation*, then the current triplet is a triplet of $SU(2)_L$, the *weak isotopic spin*.

The right handed fermions are singlet for the $SU(2)_L$, thus

$$e_R \rightarrow e'_R = e_R. \quad (1.2.9)$$

Since we are considering the global transformations, we have no interaction, so the Lagrangian reads

$$\mathcal{L} = \bar{e} i \gamma^\mu \partial_\mu e + \bar{\nu} i \gamma^\mu \partial_\mu \nu \equiv \bar{\chi}_L i \gamma^\mu \partial_\mu \chi_L + \bar{e}_R i \gamma^\mu \partial_\mu e_R; \quad (1.2.10)$$

for now we are bounded to set $m_e = 0$, in fact the mass term couples right and left fermion’s components and it is not $SU(2)_L$ invariant. In 1973, experiments detected events of the type

$$\bar{\nu}_\mu e^- \rightarrow \bar{\nu}_\mu e^- \quad (1.2.11)$$

$$\begin{cases} \nu_\mu N \rightarrow \nu_\mu X \\ \bar{\nu}_\mu N \rightarrow \bar{\nu}_\mu X \end{cases} \quad (1.2.12)$$

which are evidence of a neutral current. Further investigations yielded that the neutral weak current is predominantly $V - A$ (i.e. left-handed) but not purely $V - A$ so the

$J_\mu^{(3)}(x)$ current introduced above can not be used as it involves only left handed fermions. We know a neutral current that mixes left and right components namely the electromagnetic current

$$J_\mu \equiv eJ_\mu^{(em)} = e\bar{\psi}\gamma_\mu Q\psi \quad (1.2.13)$$

where Q is the charge operator with eigenvalue $Q = -1$ for the electron. Q is the generator of the $U(1)_{(em)}$ group. So we have an isospin triplet and we have included the right hand components, the isospin singlet, what we want to do, is to combine them and define the hypercharge operator

$$Y = 2(Q - T_3) \rightarrow Q = T_3 + \frac{Y}{2}, \quad (1.2.14)$$

for the current we have

$$J_\mu^{(em)} = J_\mu^{(3)} + \frac{1}{2}J_\mu^Y \quad (1.2.15)$$

where

$$J_\mu^Y = \bar{\psi}\gamma_\mu Y\psi \quad (1.2.16)$$

so, by analogy, the hypercharge Y generates a $U(1)_Y$ symmetry, and, as it is a $SU(2)_L$ singlet, leaves (1.2.10) invariant under the transformations

$$\begin{aligned} \chi_L(x) &\rightarrow \chi'_L(x) = e^{i\beta Y} \chi_L(x) \equiv e^{i\beta y_L} \chi_L \\ e_R(x) &\rightarrow e'_R(x) = e^{i\beta Y} e_R(x) \equiv e^{i\beta y_R} e_R. \end{aligned} \quad (1.2.17)$$

We thus have incorporated the electromagnetic interactions extending the group to $SU(2)_L \times U(1)_Y$ and instead of having a single symmetry group we have a direct product of groups, each with his own *coupling constant*, so, in addition to e we will have another coupling to be found. Since we have a direct product of symmetry groups, the generators of $SU(2)_L$, T_i , and the generators of $U(1)_Y$, Y commute, the commutation relations are

$$[T_+, T_-] = 2T_3 \quad ; \quad [T_3, T_\pm] = \pm T_\pm \quad ; \quad [Y, T_\pm] = [Y, T_3] = 0, \quad (1.2.18)$$

member of the same isospin triplet, have same hypercharge eigenvalue; the relevant quantum numbers are summarized in the table 1.1.

Lepton	T	$T^{(3)}$	Q	Y	Quark	T	$T^{(3)}$	Q	Y
ν_e	$\frac{1}{2}$	$\frac{1}{2}$	0	-1	u_L	$\frac{1}{2}$	$\frac{1}{2}$	$\frac{2}{3}$	$\frac{1}{3}$
e_L^-	$\frac{1}{2}$	$-\frac{1}{2}$	-1	-1	d_L	$\frac{1}{2}$	$-\frac{1}{2}$	$-\frac{1}{2}$	$\frac{1}{3}$
					u_R	0	0	$\frac{2}{3}$	$\frac{4}{3}$
e_R^+	0	0	-1	-2	d_R	0	0	$-\frac{1}{3}$	$-\frac{2}{3}$

Table 1.1: Weak Isospin and Hypercharge Quantum Numbers of Leptons and Quarks

1.2.2 Electro-Weak Interactions

As stated before, interactions are mediated by a gauge boson, we now want to find out those for the electroweak interaction, to this end let us consider *local* gauge transformations

$$\begin{aligned} \chi_L &\rightarrow \chi'_L = e^{i\vec{\epsilon}(x) \cdot \vec{T} + i\beta(x)Y} \chi_L \\ \psi_R &\rightarrow \psi'_R = e^{i\beta(x)Y} \psi_R, \end{aligned} \quad (1.2.19)$$

introducing four gauge bosons, $W_\mu^{(1)}, W_\mu^{(2)}, W_\mu^{(3)}, B_\mu$ (same as the number of generators) and the *covariant derivative*

$$\begin{aligned} D_\mu \chi_L &= (\partial_\mu + ig \frac{\vec{\tau}}{2} \cdot \vec{W}_\mu(x) + i \frac{g'}{2} y_L B_\mu(x)) \chi_L \\ &= (\partial_\mu + ig \frac{\vec{\tau}}{2} \cdot \vec{W}_\mu(x) - i \frac{g'}{2} B_\mu(x)) \chi_L \\ D_\mu \psi_R &= (\partial_\mu + i \frac{g'}{2} y_R B_\mu(x)) \psi_R \\ &= (\partial_\mu - i \frac{g'}{2} B_\mu(x)) e_R \end{aligned} \quad (1.2.20)$$

the Lagrangian (1.2.10) reads

$$\begin{aligned} \mathcal{L} &= \bar{\chi}_L i \gamma \partial \chi_L + \bar{e}_R i \gamma \partial e_R - g \bar{\chi}_L \gamma^\mu \frac{\vec{\tau}}{2} \chi_L \vec{W}_\mu + \frac{g'}{2} (\bar{\chi}_L \gamma^\mu \chi_L + 2 \bar{e}_R \gamma^\mu e_R) B_\mu \\ &\quad - \frac{1}{4} \vec{W}_{\mu\nu} \vec{W}^{\mu\nu} - \frac{1}{4} B_{\mu\nu} B^{\mu\nu} \end{aligned} \quad (1.2.21)$$

where

$$\begin{aligned} \vec{W}_{\mu\nu} &= \partial_\mu \vec{W}_\nu - \partial_\nu \vec{W}_\mu - g \vec{W}_\mu \times \vec{W}_\nu \\ B_{\mu\nu} &= \partial_\mu B_\nu - \partial_\nu B_\mu \end{aligned} \quad (1.2.22)$$

are the kinetic plus non abelian interaction term for the $SU(2)_L$ symmetry (first equation) and the kinetic term for the abelian symmetry group $U(1)_Y$. We can now split the Lagrangian terms to find out the field of the vector bosons coupled to the charged current and to the neutral current.

Charged Currents Interaction Let us consider the term

$$\mathcal{L}_{int}^{ew} = -g \bar{\chi}_L \gamma^\mu \frac{\vec{\tau}}{2} \chi_L \vec{W}_\mu + \frac{g'}{2} \bar{\chi}_L \gamma^\mu \chi_L B_\mu + g' \bar{e}_R \gamma^\mu e_R B_\mu \quad (1.2.23)$$

defining

$$W_\mu^\pm = \frac{1}{\sqrt{2}} W_\mu^{(1)} \mp i W_\mu^{(2)} \quad (1.2.24)$$

we can write

$$\mathcal{L}^{CC} = -\frac{g}{\sqrt{2}} (J_\mu^{(+)} W^{-\mu} + J_\mu^{(-)} W^{+\mu}) \quad (1.2.25)$$

and recognize two charged vector bosons with coupling given by “ g ”.

Neutral Current Interaction The relevant term left to consider for what concerns the electroweak currents is

$$\mathcal{L}^{NC} = -g J_\mu^{(3)} W^{(3)\mu} - \frac{g'}{2} J_\mu^Y B^\mu, \quad (1.2.26)$$

the electromagnetic interaction, $-ie J^{(em)\mu} A_\mu$, is embedded in this expression as will become clear considering the *spontaneously broken symmetry* phenomena, for now, is sufficient to define

$$\begin{aligned} W_\mu^{(3)} &= \cos \theta_w Z_\mu + \sin \theta_w A_\mu \\ B_\mu &= -\sin \theta_w Z_\mu + \cos \theta_w A_\mu \end{aligned} \quad (1.2.27)$$

and invert to get

$$\begin{aligned} A_\mu &= \sin \theta_w W_\mu^{(3)} + \cos \theta_w B_\mu \\ Z_\mu &= \cos \theta_w W_\mu^{(3)} - \sin \theta_w B_\mu \end{aligned} \quad (1.2.28)$$

where θ_w is the electroweak *mixing angle*. Plugging this into (1.2.26) and rearranging terms

$$\begin{aligned} \mathcal{L}^{NC} &= -[(g \sin \theta_w J_\mu^{(3)} + \frac{g'}{2} \cos \theta_w J_\mu^Y) A^\mu \\ &\quad + (g \cos \theta_w J_\mu^{(3)} - \frac{g'}{2} \sin \theta_w J_\mu^Y) Z^\mu] \end{aligned} \quad (1.2.29)$$

since A^μ is the photon field, the first parenthesis must be identified with the electromagnetic current, thus

$$-(g \sin \theta_w J_\mu^{(3)} + \frac{g'}{2} \cos \theta_w J_\mu^Y) A^\mu = -e J_\mu^{(em)} A^\mu \equiv -e (J_\mu^{(3)} + \frac{J_\mu^Y}{2}) A^\mu \quad (1.2.30)$$

from which we get the relation

$$g \sin \theta_w = g' \cos \theta_w = e \quad (1.2.31)$$

and so we can rewrite (1.2.26),

$$\mathcal{L}^{NC} = -\frac{g}{\cos \theta_w} [J_\mu^{(3)} - \sin^2 \theta_w J_\mu^{(em)}] Z^\mu \quad (1.2.32)$$

so that Z^μ can be identified with the field for the neutral vector boson.

1.3 The Higgs mechanism

Up to now, we have massless gauge vector bosons, in fact no term such as $M^2 B_\mu B^\mu / 2$ appear in the Lagrangian (1.2.21), but this kind of terms are not gauge invariant and thus we can not just add them or we will end up with troubles later when trying to renormalize the theory.

A gauge invariant way to recover the fermions and bosons masses, is to spontaneously brake the local $SU(2)_L \times U(1)_Y$ electroweak symmetry.

1.3.1 Non Abelian Spontaneously Broken Symmetry

Let us consider a local symmetry breaking and refer to [1] for a more complete explanation. Be ϕ a complex scalar field,

$$\mathcal{L} = (\partial_\mu \phi^*)(\partial_\mu \phi) - \underbrace{\mu^2 \phi^* \phi - \lambda (\phi^* \phi)^2}_{V(\phi^* \phi)} \quad (1.3.1)$$

setting

$$\begin{aligned} \phi &= \frac{\phi_1 + i\phi_2}{\sqrt{2}} \\ \phi^* &= \frac{\phi_1 - i\phi_2}{\sqrt{2}} \end{aligned} \quad (1.3.2)$$

we get

$$\mathcal{L} = \frac{1}{2}(\partial_\mu \phi_1)^2 + \frac{1}{2}(\partial_\mu \phi_2)^2 - \frac{\mu^2}{2}(\phi_1^2 + \phi_2^2) - \frac{\lambda}{4}(\phi_1^2 + \phi_2^2)^2 \quad (1.3.3)$$

the gauge transformations are

$$\begin{cases} \phi(x) \rightarrow \phi'(x) = e^{i\epsilon} \phi(x) \\ \phi^\dagger(x) \rightarrow \phi'^\dagger(x) = e^{-i\epsilon} \phi^\dagger(x). \end{cases} \quad (1.3.4)$$

There are two possible choices for the potential

- $\mu^2 > 0$, which gives a stable configuration around $|\phi| = 0$.
- $\mu^2 < 0$, which gives a circle of minima such that $\phi_1^2 + \phi_2^2 = v^2$, with $v^2 = -\mu^2/\lambda$.
This minima are not gauge invariant, in fact

$$\phi_0 = \langle 0|\phi|0 \rangle \rightarrow \frac{v}{\sqrt{2}} e^{i\alpha} \quad \text{if} \quad \phi \rightarrow e^{i\alpha} \phi \quad (1.3.5)$$

To get the particle interaction we make a perturbative expansion around one minimum, we chose one, for example $\alpha = 0$, for which $\phi_1 = v$ and $\phi_2 = 0$ and introduce the two perturbations $\eta(x)$ and $\xi(x)$ so that

$$\phi(x) = \frac{1}{\sqrt{2}} \overbrace{v + \xi(x)}^{\phi_1} + i \overbrace{\eta(x)}^{\phi_2} \quad (1.3.6)$$

and plug them in the Lagrangian (1.3.3) to obtain

$$\begin{aligned} \mathcal{L}'(\xi, \eta) &= \frac{1}{2}(\partial_\mu \xi)^2 + \frac{1}{2}(\partial_\mu \eta)^2 - \frac{1}{2}(-2\mu^2)\eta^2 \\ &\quad - \lambda v(\eta^2 + \xi^2)\eta - \frac{1}{4}(\eta^2 + \xi^2)^4 + \dots \end{aligned} \quad (1.3.7)$$

as we can see, the third term looks like a mass term so that the field η has mass $m_\eta^2 = -2\mu^2$ while we have no mass term for the field ξ .

This “trick” to give mass to one of the gauge field, is the *braking of the symmetry*. In fact, by choosing one particular vacuum among the infinite ones, we lost our gauge invariance; moreover, we ended up with a scalar gauge boson, known as *Goldstone boson*. We need to find a way to recover the masses of the gauge bosons in a gauge invariant way by getting rid of massless scalar fields; the solution is the topic of the very next section. next section.

1.3.2 The Higgs Mechanism

Consider now a local gauge $SU(2)$ symmetry, the field transformations are

$$\phi(x) \rightarrow \phi'(x) = e^{i\sum_{k=1}^3 \epsilon^k T^k} \phi(x), \quad (1.3.8)$$

where $T^k = \frac{\tau^k}{2}$ and $[T^i, T^j] = i\epsilon^{ijk} T^k$ with $i, j, k = 1, 2, 3$. To achieve invariance for the Lagrangian

$$\mathcal{L} = (\partial_\mu \phi)^\dagger (\partial^\mu \phi) - \mu^2 \phi^\dagger \phi - \lambda(\phi^\dagger \phi)^2, \quad (1.3.9)$$

where

$$\phi \equiv \begin{pmatrix} \phi_i \\ \phi_j \end{pmatrix} = \frac{1}{\sqrt{2}} \begin{pmatrix} \phi_1 + i\phi_2 \\ \phi_3 + i\phi_4 \end{pmatrix}, \quad (1.3.10)$$

we need to introduce the covariant derivative

$$D_\mu = \partial_\mu + ig \frac{\vec{\tau}}{2} \cdot \vec{W}_\mu(x). \quad (1.3.11)$$

In the case of infinitesimal transformations, the fields transform like

$$\phi(x) \rightarrow \phi'(x) \simeq (1 + i\vec{\epsilon}(x) \cdot \frac{\vec{\tau}}{2})\phi(x) \quad (1.3.12)$$

while the gauge bosons transformations are

$$\vec{W}_\mu(x) \rightarrow \vec{W}_\mu(x) - \frac{1}{g}\partial_\mu \vec{\epsilon}(x) - \vec{\epsilon}(x) \times \vec{W}_\mu(x). \quad (1.3.13)$$

Replacing everything in the Lagrangian we obtain

$$\mathcal{L} = (\partial_\mu \phi + ig \frac{\vec{\tau}}{2} \cdot \vec{W}_\mu \phi)^\dagger (\partial_\mu \phi + ig \frac{\vec{\tau}}{2} \cdot \vec{W}_\mu \phi) - V(\phi) - \frac{1}{4} \vec{W}_{\mu\nu} \cdot \vec{W}^{\mu\nu}, \quad (1.3.14)$$

where the potential is given by

$$V(\phi) = \mu^2 \phi^\dagger \phi + \lambda (\phi^\dagger \phi)^2 \quad (1.3.15)$$

and the kinetic term is

$$\vec{W}_{\mu\nu} = \partial_\mu \vec{W}_\nu - \partial_\nu \vec{W}_\mu - g \vec{W}_\mu \times \vec{W}_\nu. \quad (1.3.16)$$

We are interested in the case of the spontaneously broken symmetry, thus $\mu^2 < 0$ and $\lambda > 0$. The minima of the potential lie on

$$\phi^\dagger \phi = \frac{1}{2}(\phi_1^2 + \phi_2^2 + \phi_3^2 + \phi_4^2) = -\frac{\mu^2}{2\lambda} \quad (1.3.17)$$

and we have to choose one of them, let it be

$$\phi_1 = \phi_2 = \phi_4 = 0, \quad \phi_3^2 = -\frac{\mu^2}{\lambda} \equiv v^2. \quad (1.3.18)$$

To expand ϕ around this particular vacuum

$$\phi_0 \equiv \frac{1}{\sqrt{2}} \begin{pmatrix} 0 \\ v \end{pmatrix} \quad (1.3.19)$$

it is sufficient to substitute the expansion

$$\phi(x) = \frac{1}{\sqrt{2}} \begin{pmatrix} 0 \\ v + h(x) \end{pmatrix} \quad (1.3.20)$$

in the Lagrangian (1.3.14) in order to get rid of the, unobserved, Goldstone bosons and retain only one neutral scalar field, the *Higgs field*.

1.3.3 Masses for the W^\pm and Z^0 Gauge Bosons

The gauge bosons masses are generated simply substituting the vacuum expectation value, ϕ_0 , in the Lagrangian, the relevant term is

$$\begin{aligned}
 \left| \left(g \frac{\vec{\tau}}{2} \cdot \vec{W}_\mu + \frac{g'}{2} B_\mu \right) \phi \right|^2 &= \\
 &= \frac{1}{8} \left| \begin{pmatrix} gW_\mu^3 + g'B_\mu & g(W_\mu^1 - iW_\mu^2) \\ g(W_\mu^1 + iW_\mu^2) & -gW_\mu^3 + g'B_\mu \end{pmatrix} \begin{pmatrix} 0 \\ v \end{pmatrix} \right|^2 \\
 &= \frac{1}{8} v^2 g^2 [(W_\mu^1)^2 + (W_\mu^2)^2] + \frac{1}{8} v^2 (g'B_\mu - gW_\mu^3)(g'B_\mu - gW_\mu^3) \\
 &= \left(\frac{1}{2} g v \right)^2 W_\mu^+ W_\mu^- + \frac{1}{8} v^2 \begin{pmatrix} W_\mu^3 & B_\mu \end{pmatrix} \begin{pmatrix} g^2 & -gg' \\ -gg' & g'^2 \end{pmatrix} \begin{pmatrix} W_\mu^3 \\ B_\mu \end{pmatrix}
 \end{aligned} \tag{1.3.21}$$

having used $W^\pm = (W^1 \mp iW^2)/\sqrt{2}$. The mass term, lead us to conclude that

$$M_W = \frac{1}{2} g v. \tag{1.3.22}$$

The remaining term is off diagonal

$$\begin{aligned}
 \frac{1}{8} v^2 [g^2 (W_\mu^3)^2 - 2gg' W_\mu^3 B_\mu + g'^2 B_\mu^2] &= \frac{1}{8} v^2 [gW_\mu^3 - gB_\mu]^2 \\
 &\quad + 0 \quad [g'W_\mu^3 - g'B_\mu]^2
 \end{aligned} \tag{1.3.23}$$

but one can diagonalize and find that

$$\begin{aligned}
 A^\mu &= \frac{g'W_\mu^3 + gB_\mu}{\sqrt{g^2 + g'^2}} \\
 Z^\mu &= \frac{gW_\mu^3 - g'B_\mu}{\sqrt{g^2 + g'^2}}
 \end{aligned} \tag{1.3.24}$$

with $M_A = 0$ and $M_Z = v\sqrt{g^2 + g'^2}/2$ which are the photon and neutral weak vector boson fields. Thus the mass eigenstates are a massless vector boson, A_μ and a massive gauge boson Z_μ .

We have shown in this section how the Higgs mechanism can be applied to give mass to the gauge bosons of the electroweak model.

1.4 The hierarchy problem and naturalness

The *naturalness criterion* states that one such [dimensionless and measured in units of the cut-off] parameter is allowed to be much smaller than unity only if setting it to zero increases the symmetry of the theory. If this does not happen, the theory is unnatural [2].

There are two important concepts in physics that enter in the formulation of the naturalness principle, symmetries and effective field theories. *Symmetries* are closely connected to conservation laws, moreover theory parameters that are protected by a symmetry, if smaller than the unit, are not problematic according to the naturalness criterion. *Effective field theories* are a sort of simplification of a more general theory

that use less parameters to describe the dynamics of particles with energies less than a cut-off scale Λ .

Let us now consider the strength of the gravitational force, characterized by the Newton's constant, G_N and the weak force, characterized by the Fermi's constant G_F , if we take the ratio of these we get:

$$\frac{G_F \hbar^2}{G_N c^2} = 1.738 \times 10^{33}. \quad (1.4.1)$$

The reason why this number is worth some attention is that theory parameters close to the order of the unit in the SM, may be calculated in a more fundamental theory, if any, using fundamental constants like π or e while very big numbers may not have such a simple mathematical expression and thus may lead to uncover new properties of the fundamental theory.

This number becomes even more interesting if we consider quantum effects. *Virtual particles* are not really particles but rather disturbances in a field, these disturbances are off-shell ($E \neq m^2 + p^2$) and according to the *uncertainty principle*, $\Delta t \Delta E \geq \hbar/2$, can appear out of nothing for a short time that depends on the energy of the virtual particle; according to quantum field theory, the vacuum is populated with such disturbances. The Higgs field, has the property to couple with other SM particles with a strength proportional to their mass. Now all these virtual particles have a mass determined by the available energy Λ and when the Higgs field travels through space, it couples with these virtual particles and, due to quantum corrections, its motion is affected and its invariant mass squared gets a contribution proportional to Λ :

$$\delta m_H^2 = k \Lambda^2, \text{ with } k = \frac{3G_F}{4\sqrt{2}\pi^2} (4m_t^2 - 2m_W^2 - m_Z^2 - m_H^2). \quad (1.4.2)$$

Since $k \approx 10^{-2}$ [3], the value of Higgs' mass $m_H \sim G_F^{-1/2}$, should be close to the maximum energy scale Λ and if we assume this to be the Plank scale $M_{Pl} = G_N^{-1/2}$, the ration G_F/G_N , should be close to the unity which contradicts eq. (1.4.1), this goes by the name of *hierarchy problem*.

The large quantum corrections in (1.4.2) are mainly due to the fact that in the SM, there is no symmetry protecting the mass of the Higgs' field. Supersymmetry (SUSY), among other things, is capable of solving the hierarchy problem by canceling out the quantum corrections that bring m_H close to Λ thus restoring the naturalness of the SM.

Chapter 2

Experimental apparatus

2.1 The large hadron collider

Insert this part

2.2 The ATLAS detector

The ATLAS detector ...

2.2.1 The inner detector

The inner detector (ID) is designed to provide good track reconstruction, precise momentum resolution and both primary and secondary vertex measurements above a nominal p_T threshold of 0.5 GeV and within the pseudorapidity $|\eta| < 2.5$. It also provides electron identification over $|\eta| < 2.0$ for energies between 0.5 GeV and 150 GeV[4]. The ID is 6.2 m long and has a radius of about 1.1 m, it is surrounded by a solenoidal magnetic field of 2 T. Its layout is schematized in Figure 2.1 and, as can be seen, it is composed of three sub-detectors.

At the inner radius the *pixel detector* mostly determines the position of primary and secondary vertex. The silicon sensors are 250 μm thick detectors that operate with an initial bias voltage of ~ 150 V that, due to the high radiation level, will increase up to 600 V after 10 years of operation to maintain a good charge collection.

In the middle layer of the ID the *semiconductor tracker* (SCT) is designed to give eight precision measurements per track which contributes to determine the primary and secondary vertex position and momentum measurements. The silicon sensors are $285 \pm 15 \mu\text{m}$ thick and initially operates with a bias voltage of ~ 150 V which will increase up to 350 V after ten years of operation for good charge collection.

The last layer of the ID is the *transition radiation tracker* (TRT), it contributes to tracking and identification of charged particles. It consists of drift (straw) tubes, 4 mm in diameter with a 31 μm wire in the center of each straw, filled with a gas mixture of 70% Xe, 27% CO₂ and 3% O₂. These tubes substantially act like proportional counters where the tube is the cathode and kept at -1.5 kV and the wire is the anode and grounded. When a charged particle cross one tube, leaves a signal; the set of signals in the tubes, reconstructs to a track which represents the path of the crossing object. The space between the straw tubes is filled with material with different refraction index,

this causes charged particles crossing it to emit transition radiation thus leading to some straw to have a much stronger signal. The transition radiation depends on the speed of the particles which in turn depends on the initial energy and the mass of the particles thus lighter particles will have higher transition energy and stronger signal in the straw tubes. Tracks with several strong signal straw, can be identified as belonging to electrons (the lightest charged particle).

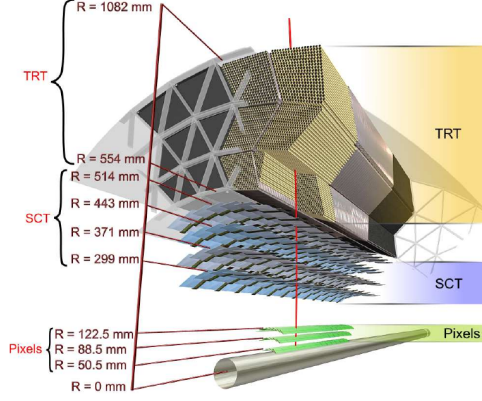


Figure 2.1: Schematic view of a charged track of 10 GeV p_T that traverses the different ID sub-detectors. After traversing the beryllium pipe, the track passes through the three cylindrical silicon-pixel layers, the four layers of silicon-microstrip sensors (SCT) and the approximately 36 straws contained in the TRT within their support structure.

2.2.2 The calorimeter

The main purpose of a calorimeter is to measure the energy of electrons, photons and hadrons by mean of materials capable of completely absorb the energy of the incoming particles transforming it in some measurable quantity. Calorimeters can be classified in two categories, *electromagnetic* (EM) and *hadronic* depending on the particle they are designed to detect. The EM calorimeters are mainly used to detect photons and electrons while the task of hadronic calorimeters is to identify hadrons. Both types of calorimeters can be further divided into *sampling calorimeters* and *homogeneous calorimeters*. Sampling calorimeters alternates layers of a dense material used to absorb the energy of incident particles (absorber) and an active material to collect the signal. The interaction between the particles and the absorber produces a shower of secondary particles with progressively degraded energy which is deposited in the active material in form of charge or light that can be converted into energy. Homogeneous calorimeters use only one material that serves both as an absorber and an active material[5].

The ATLAS calorimeter is a sampling calorimeter covering up the $|\eta| < 4.9$ region the large η coverage, ensures a good missing transverse momentum measurement (see Section 3.1.5); an illustration of the system is shown in Figure 2.2.

The EM calorimeter has a barrel and two end-caps, covering the $|\eta| < 1.475$ and $1.375 < |\eta| < 3.2$ region respectively. It uses liquid Argon (LAr) as active material and lead as absorber in an accordion geometry that provides ϕ symmetry without azimuthal cracks. In the region $|\eta| < 1.8$ a presampler consisting of a LAr active region is used to correct for electrons and photons energy loss upstream of the calorimeter.

There are then three hadronic calorimeters: the *Tile Calorimeter* (TileCal), the *Hadronic End-cap Calorimeter* (HEC) and the *LAr Forward Calorimeter* (FCal). The TileCal barrel and extended barrels cover the $|\eta| < 1.0$ and $0.8 < |\eta| < 1.7$ and uses steel as absorber and scintillating tiles connected to photomultiplier tubes through wavelength shifting fibers for readout as an active material. The HEC covers the $1.5 < |\eta| < 3.2$ region and, to avoid drops in material density at the transition, it overlaps slightly with the FCal that covers the $3.1 < |\eta| < 4.9$.

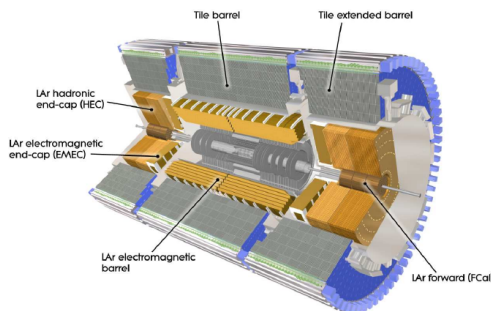


Figure 2.2: Cut-away view of the ATLAS calorimeter system.

2.2.3 The muon spectrometer

The Muon Spectrometer (MS) is designed to identify muons and measure their momentum. It is divided in four sub-detectors, the Monitored Drift Tubes (MDT), the Cathode Strip Chambers (CSC), the Resistive Plate Chambers (RPC), and the Thin Gap Chamber (TGC) that. The sub-detectors are immersed in a magnetic field generated by three different toroidal magnets, a barrel toroid covering the $|\eta| < 1.4$ region and two end-caps magnets at $1.6 < |\eta| < 2.7$, which produces a field almost perpendicular to the muon tracks.

The MDT covers the $|\eta| < 2.7$ region and provides a precise measurement of the track coordinates in the principal bending direction of the magnetic field. It uses drift tubes filled with an Ar (93%) and CO₂ (3%) gas mixture and a tungsten-rhenium wire at 3080 V potential as anode. To reconstruct the muon trajectory, the drift time of the ionized charges is used to determine the minimum distance between the wire and the muon. The CSC covers the $2.0 < |\eta| < 2.7$ region and is a multi-wire proportional chamber with cathodes segmented in strips, one perpendicular to the anode wire, providing the precision coordinate, and the other parallel to it (giving the transverse coordinate).

The RPC and the TGC cover the $|\eta| < 1.05$ and $1.05 < |\eta| < 2.7$ regions respectively. They contribute to the Level 1 trigger providing bunch-crossing identification, it allows to select high and low p_T tracks and measure the muon coordinate in the direction orthogonal to that determined by MDT and CSC.

2.2.4 The forward detectors

Insert this part

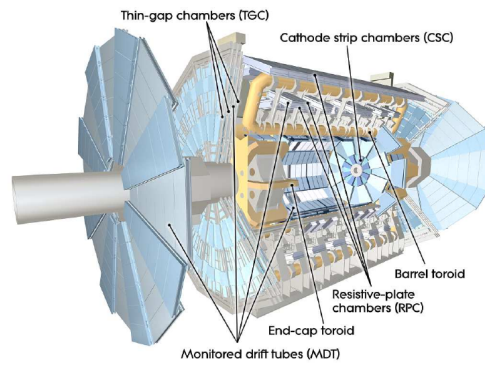


Figure 2.3: Cut-away view of the ATLAS muon spectrometer.

2.2.5 Track reconstruction

Write here briefly about track reconstruction and most importantly about the impact parameters d_0 and z_0 .

2.2.6 The trigger system

Insert this part

Chapter 3

Physical objects reconstruction

3.1 Lepton reconstruction and identification

This analysis uses electrons, muons, jets and missing transverse momentum (E_T^{miss}). Two types of electrons, muons and jets are also defined: *baseline* and *good*, where the former one is used for overlap removal and preselection while the latter for selecting the objects used to define the signal and control regions. In the following a brief introduction to the identification criteria of these objects is presented.

3.1.1 Primary Vertex

Insert this part

3.1.2 Overlap removal

Insert this part

3.1.3 Electrons

Electrons are identified in the central part of the ATLAS detector ($|\eta| < 2.47$) by an energy deposit in the electromagnetic calorimeter and an associated track in the inner detector. Signal electrons are defined as prompt electrons coming from the decay of a W , Z boson or a top quark while background electrons come from hadronic jets, photon conversion and semi-leptonic heavy flavor hadron decay. A likelihood discriminator is formed using the shower shape in the EM calorimeter, the track-cluster matching, some of the track quality distributions from signal and background simulation and cuts on the number of hits in the ID. Cuts that depends on $|\eta|$ and E_T on the likelihood estimator allow to distinguish between signal and background electrons.

Electron identification efficiencies are measured in pp collisions data and compared to efficiencies measured in $Z \rightarrow ee$ simulations. Signal electrons can furthermore be selected with different sets of cuts for the likelihood-based criteria with $\sim 95\%$, $\sim 90\%$ and $\sim 80\%$ efficiency for electrons with $p_T \sim 40$ GeV. The different criteria are referred to as *loose*, *medium* and *tight* operating points respectively[6] where, for example, a tight criterion lead to a higher purity of signal electrons.

In this analysis, the *baseline electrons* are selected requiring a transverse energy $E_T > 20$ GeV, $|\eta| < 2.47$, to satisfy the *loose* likelihood selection criteria. Furthermore, it is required that no dead EM calorimeter front-end board (FEB) or high voltage (HV) channels in the calorimeter cluster are present and that the baseline electron passes the OR. The baseline electron criteria is used to veto electrons used in the muon control regions and the signal region definition. In addition to all the baseline criteria, the *good electron* definition requires the electrons to satisfy the *tight* likelihood selection criteria, the electron track $d_0/\sigma_{d0} < 5$ mm and $|z_0| < 0.5$ mm and the *LooseTrackOnly* electron isolation criteria.

Electron Definition	
Baseline electron	Good electron
$E_T > 20$ GeV	<i>baseline</i>
$ \eta < 2.47$	<i>tight</i>
<i>loose</i>	$d_0/\sigma_{d0} < 5$ mm
No dead FEB in the EM calo cluster	$ z_0 < 0.5$ mm
No dead HV in the EM calor cluster	<i>LooseTrackOnly</i>
passes the OR	

Table 3.1: Monojet electron definition

3.1.4 Jets

Insert this part

3.1.5 Missing transverse energy

Insert this part

3.1.6 Muons

Insert this part

Chapter 4

The Monojet signature

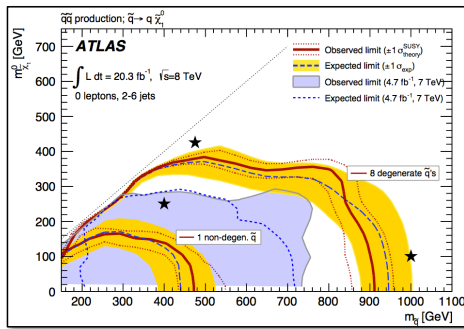
4.1 Motivation

Events with an energetic jet p_T and large E_T^{miss} in the final state, constitute a clean signature for new physics searches at hadron colliders. Signals that can be studied with this experimental signature include the production of WIMPS, the ADD model for large extra dimensions and SUSY.

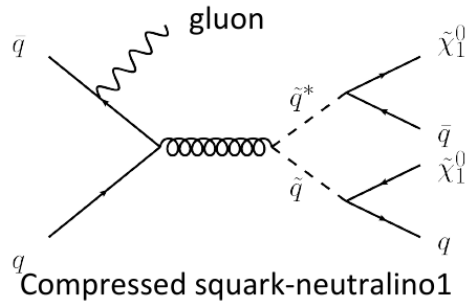
Fix this part

If the mass difference between the sparticles is small, the sensitivity to new physics signal of many standard SUSY searches is reduced due to the low amount of missing energy and the corresponding low transverse momentum of the associated jets. (why is that so? Try to think and find out) If the event has an ISR, the amount of missing energy and the corresponding transverse momentum jets will be large leading thus to a clean signature for the monojet

It is possible to estimate, from eq. (1.4.2), the scale at which new physics is expected. Using $m_H = 125$ GeV[7], we get that $\Lambda \approx 1$ TeV; thus, if the naturalness criterion holds, we expect the two main experiments at LHC, ATLAS [4] and CMS [8], to find signal for new physics at the TeV scale.



(a)



(b)

Figure 4.1

4.2 Event Selection

The search is carried out in pp collisions using the data collected by the ATLAS experiment during the 2015 Run II corresponding to a total integrated luminosity of 3.2 fb^{-1} .

Appendix A

Some title

Bibliography

- [1] F. Halzen and A. D. Martin. *Quark and Leptons: An introductory Course in Modern Particle Physics*. John Wiley & Sons INC, 1984.
- [2] G. 't Hooft. *Recent Developments in Gauge Theories*. Plenum Press, 1979.
- [3] Gian Francesco Giudice. “Naturally Speaking: The Naturalness Criterion and Physics at the LHC”. In: (2008). arXiv: [0801.2562 \[hep-ph\]](#).
- [4] The ATLAS Collaboration. “The ATLAS Experiment at the CERN Large Hadron Collider”. In: *Journal of Instrumentation* 3.08 (2008), S08003. URL: <http://stacks.iop.org/1748-0221/3/i=08/a=S08003>.
- [5] C. W. Fabjan and F. Gianotti. “Calorimetry for particle physics”. In: *Rev. Mod. Phys.* 75 (2003), pp. 1243–1286. DOI: [10.1103/RevModPhys.75.1243](#).
- [6] *Electron identification measurements in ATLAS using $\sqrt{s} = 13$ TeV data with 50 ns bunch spacing*. Tech. rep. ATL-PHYS-PUB-2015-041. Geneva: CERN, Sept. 2015. URL: <https://cds.cern.ch/record/2048202>.
- [7] K. A. Olive et al. “Review of Particle Physics”. In: *Chin. Phys.* C38 (2014), p. 090001. DOI: [10.1088/1674-1137/38/9/090001](#).
- [8] The CMS Collaboration. “The CMS experiment at the CERN LHC”. In: *Journal of Instrumentation* 3.08 (2008), S08004. URL: <http://stacks.iop.org/1748-0221/3/i=08/a=S08004>.